Icefield Breezes: Mesoscale Diurnal Circulation in the Atmospheric Boundary Layer Over an Outlet of the Columbia Icefield, Canadian Rockies

J P Conway, W D Helgason, J W Pomeroy, Jean Emmanuel Sicart

JGR Atmospheres

RESEARCH ARTICLE
10.1029/2020JD034225

Icefield Breezes: Mesoscale Diurnal Circulation in the Atmospheric Boundary Layer Over an Outlet of the Columbia Icefield, Canadian Rockies

J. P. Conway[1,2], W. D. Helgason[2,3], J. W. Pomeroy[2], and J. E. Sicart[4]

[1]National Institute of Water and Atmospheric Research, Lauder, New Zealand, [2]Centre for Hydrology, University of Saskatchewan, Saskatoon, SK, Canada, [3]Department of Civil, Geological and Environmental Engineering, University of Saskatchewan, Saskatoon, SK, Canada, [4]Université Grenoble Alpes, CNRS, IRD, Grenoble INP, Institut des Géosciences de l'Environnement (IGE)—UMR 5001, Grenoble, France

Key Points:

- A well-developed mesoscale wind develops over a Columbia Icefield outlet glacier but differs from previously documented "glacier winds"
- Novel kite and radio-acoustic observations indicate strong down-glacier winds typically extend through the lowest 200 m of above-glacier ABL
- Katabatic cooling in the glacier surface boundary layer is reduced during periods with "icefield breezes" compared to periods with typical "glacier winds"

Correspondence to:
J. P. Conway,
jono.conway@niwa.co.nz

Citation:
Conway, J. P., Helgason, W. D., Pomeroy, J. W., & Sicart, J. E. (2021). Icefield breezes: Mesoscale diurnal circulation in the atmospheric boundary layer over an outlet of the Columbia Icefield, Canadian Rockies. *Journal of Geophysical Research: Atmospheres*, *126*, e2020JD034225. https://doi.org/10.1029/2020JD034225

Received 8 NOV 2020
Accepted 5 FEB 2021

Author Contributions:

Conceptualization: J. P. Conway, W. D. Helgason, J. W. Pomeroy, J. E. Sicart
Data curation: J. P. Conway, W. D. Helgason
Formal analysis: J. P. Conway
Funding acquisition: W. D. Helgason, J. W. Pomeroy
Investigation: J. P. Conway, W. D. Helgason, J. W. Pomeroy, J. E. Sicart
Methodology: J. P. Conway, W. D. Helgason, J. E. Sicart
Project Administration: W. D. Helgason, J. W. Pomeroy
Resources: W. D. Helgason, J. W. Pomeroy
Supervision: W. D. Helgason, J. W. Pomeroy
Writing – original draft: J. P. Conway

Abstract Atmospheric boundary layer (ABL) dynamics over glaciers mediate the response of glacier mass balance to large-scale climate forcing. Despite this, very few ABL observations are available over mountain glaciers in complex terrain. An intensive field campaign was conducted in June 2015 at the Athabasca Glacier outlet of Columbia Icefield in the Canadian Rockies. Observations of wind and temperature profiles with novel kite and radio-acoustic sounding systems showed a well-defined mesoscale circulation developed between the glacier and snow-free valley in fair weather. The typical vertical ABL structure above the glacier differed from that expected for "glacier winds"; strong daytime down-glacier winds extended through the lowest 200 m with no up-valley return flow aloft. This structure suggests external forcing at mesoscale scales or greater and is provisionally termed an "icefield breeze." A wind speed maximum near the surface, characteristic of a "glacier wind," was only observed during nighttime and one afternoon. Lapse rates of air temperature down the glacier centerline show the interaction of down-glacier cooling driven by sensible heat loss into the ice, entrainment and periodic disruption and warming. Down-glacier cooling was weaker in "icefield breeze" conditions, while in "glacier wind" conditions, stronger down-glacier cooling enabled large increases in near-surface temperature on the lower glacier during periods of surface boundary layer (SBL) disruption. These results raise several questions, including the impact of Columbia Icefield on the ABL and melt of Athabasca Glacier. Future work should use these observations as a testbed for modeling spatio-temporal variations in the ABL and SBL within complex glaciated terrain.

Plain Language Summary Mountain glaciers are experiencing rapid change in response to climate change. But to confidently attribute past change and predict future change, our mathematical models need to account for how glaciers modify the climate they experience. New measurements of wind and temperature have been made over an outlet glacier of the Columbia Icefield, Canadian Rockies using a novel kite-based measurement system along with an extensive set of meteorological measurements on the glacier surface and in the valley below the glacier. They show that the persistent down-glacier winds observed at the glacier surface have a different vertical structure than expected from previous observations and theory. Down-glacier winds typically cool the air next to the surface as it travels down-glacier. Here it is shown that this cooling process is more limited when the wind is strong throughout the lower valley over the glacier, compared with times when wind speed is strongest next to the glacier and weaker above. The data set presented in this paper provides an opportunity to test the models used to link glaciers and climate.

1. Introduction

Atmospheric dynamics over glaciers are of interest as they mediate the response of glacier mass balance to global and regional forcing. The contrast of snow/ice surfaces with surrounding land surfaces, complex topography and the unique geometry of valley glaciers combine to create distinctive meteorology within the mountain atmospheric boundary layer (ABL) and the glacier surface boundary layer (SBL) immediately above the glacier surface. Perhaps the most prominent feature of the glacier SBL is persistent and often strong down-glacier winds termed "katabatic" or "glacier winds" (e.g., Martin, 1975; Ohata, 1989; Streten

Writing – review & editing: J. P. Conway, W. D. Helgason, J. W. Pomeroy, J. E. Sicart

& Wendler, 1968). These winds can markedly alter the spatio-temporal distribution of air temperature over glacier surfaces from the environmental lapse rate (e.g., Ayala et al., 2015; Carturan et al., 2015; Greuell et al., 1997; Petersen et al., 2013; Shea & Moore, 2010; Troxler et al., 2020) by enabling the air next to the glacier surface to become isolated from the ABL and to cool as it travels down-glacier to lower elevations (herein referred to as down-glacier cooling) (Greuell & Böhm, 1998). These variations in SBL air temperature alter the surface energy balance and ultimately the distribution of melt (e.g., Greuell & Smeets, 2001; Petersen & Pellicciotti, 2011; Shaw et al., 2017).

Persistent down-glacier winds can originate from a range of forcings. The term "glacier winds" commonly refers to summertime winds that form when the glacier surface is melting (van den Broeke, 1997b) while "katabatic" winds can refer to both "glacier winds" and drainage flows driven by radiative losses from the surface, such as those prevalent during night-time and over Antarctica (e.g., Parish & Bromwich, 2007; Poulos & Zhong, 2008). Katabatic and "glacier winds" are buoyancy-driven flows, induced by the cooling of near-surface air by sensible heat exchange and subsequent downward transport of the dense cold air (Hoinkes, 1954; Poulos & Zhong, 2008). Previous observations of "glacier winds" found up-valley flow overlying the near-surface down-glacier flow (van den Broeke, 1997b). In addition to buoyancy-driven flows, glaciers in mountainous regions are also likely to be affected by topographic channeling of large-scale gradient winds and/or down-slope winds that are induced by dynamical interactions of the gradient wind with the topography (Jiang & Doyle, 2008).

Despite the importance of correctly representing interactions between glaciers and climate within glaciological, hydrological and meteorological models, few observations of the ABL in the few hundred meters above glacier surfaces have been made. The lack of ABL observations above mountain glaciers is primarily due to the difficulty in making measurements in these environments; the often inaccessible locations provide formidable logistical challenges, while rapid summer melt and unstable surfaces make a poor platform for ground-based remote sensing and extreme climates are a challenge for sensitive instrumentation. Observations and modeling of katabatic wind systems in Antarctica have received much attention (e.g., Bromwich et al., 1993; Parish & Bromwich, 1989; van Lipzig et al., 2004). The only large field campaign to have systematically observed the ABL in the lowest few hundreds of meters above a mid-latitude mountain glacier was the PASTEX campaign, in which multiple automatic weather stations (AWS) and a tethered balloon system were deployed on the Pasterze Glacier (Greuell et al., 1997; van den Broeke, 1997b). Similar campaigns have targeted icecaps in Iceland (Oerlemans et al., 1999; Reuder et al., 2012) and the melting edge of the Greenland Ice Sheet (van den Broeke et al., 1994). Observations of wind speed and temperature gradients within the lowest few meters of the glacier SBL have been made in various locations (e.g., Litt et al., 2017; Munro & Davies, 1977; Sicart et al., 2014) and have shown that the validity of bulk aerodynamic methods used to model turbulent heat fluxes depends on the proximity of a wind speed maximum to the glacier surface and the extent to which large-scale winds influence the glacier SBL (e.g., Litt et al., 2015; Radic et al., 2017; Smeets et al., 1998, 2000). Observations of spatial and temporal variations in surface meteorology, most commonly air temperature, have also been made over many glaciers (e.g., Ayala et al., 2015; Greuell & Böhm, 1998; Petersen & Pellicciotti, 2011; Shea & Moore, 2010), with some studies showing that spatial variability is often linked to different wind flow regimes. Owing to their strong influence on surface energetics, many recent studies have focused on the methods to extrapolate the spatial distribution of on-glacier air temperatures from on-glacier and/or off-glacier sites (e.g., Ayala et al., 2015; Carturan et al., 2015; Petersen et al., 2013; Petersen & Pellicciotti, 2011; Shaw et al., 2017, 2020; Shea & Moore, 2010; Troxler et al., 2020). Other recent studies have directly quantified the influence of wind flow regimes on spatial variability of surface heat fluxes (Mott et al., 2020; Sauter & Galos, 2016). However, most studies of the glacier SBL have usually lacked supporting observations of the ABL with which to help explain the atmospheric processes responsible for the variations observed. There are no documented observations of the ABL over an outlet glacier of an icefield—an ice mass smaller than the icecaps of for example Iceland or ice sheets of Greenland and Antarctica, but larger than a typical mountain glacier.

The lack of observations from the ABL over mountain glaciers and icefields limits the understanding and prediction of the interaction of the glacier SBL with valley and large-scale circulations in regions of complex terrain. This, in turn, prevents knowledgeable downscaling of atmospheric models and representation of mountain cryosphere-atmosphere interactions in past and future simulations. Improved ABL process

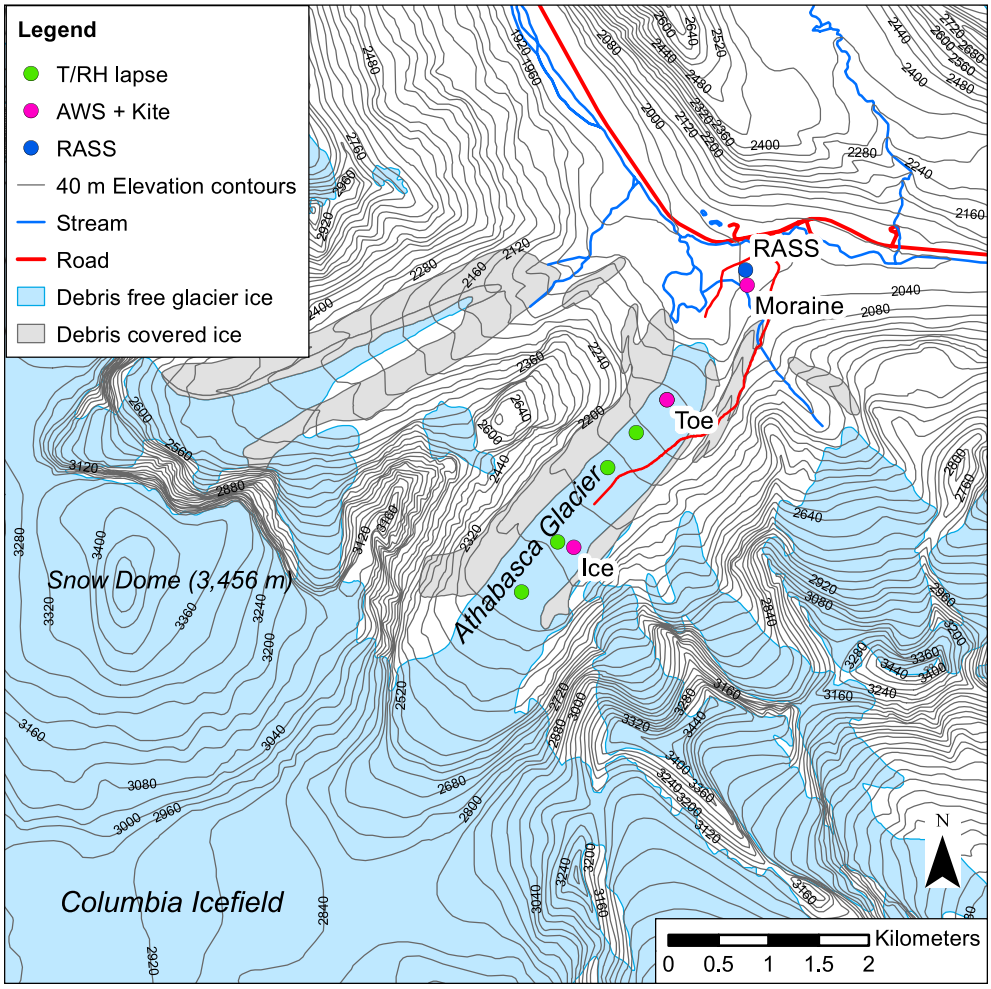

Figure 1. Map of field site and key measurement locations.

understanding and observations provide avenues to improve downscaling of near-surface meteorology from gridded climate products through the validation of dynamical downscaling efforts (e.g., Collier et al., 2013) and selection of predictor fields and algorithms used in empirical statistical downscaling (e.g., Hofer et al., 2017). To address this lack of observational datasets, an intensive campaign was initiated over the Athabasca Glacier, a mid-latitude valley glacier draining the Columbia Icefield in the Canadian Rockies Figure 1. The campaign aimed to understand the key features of the glacier-valley circulation and how they affect spatial and temporal variations in the structure of glacier ABL and SBL. This aim was addressed through the following objectives:

1. Use novel kite profiling and radio-acoustic sounding systems to document ABL conditions above the glacier and pro-glacial valley
2. Characterize the typical spatial and temporal variations in the ABL and SBL above the glacier tongue and ice-free valley during fair weather
3. Provide the basis for meteorological modeling to (a) understand the drivers of the observed circulation and (b) resolve the spatio-temporal variations in SBL climate in complex glaciated terrain

This study addresses objectives 1 and 2, as well as providing an initial assessment of the drivers of the observed glacier-valley circulation. Further, it describes ABL development downwind of an icefield for the first time. Future work should aim to test the ability of mesoscale meteorological models to simulate the processes observed during the campaign.

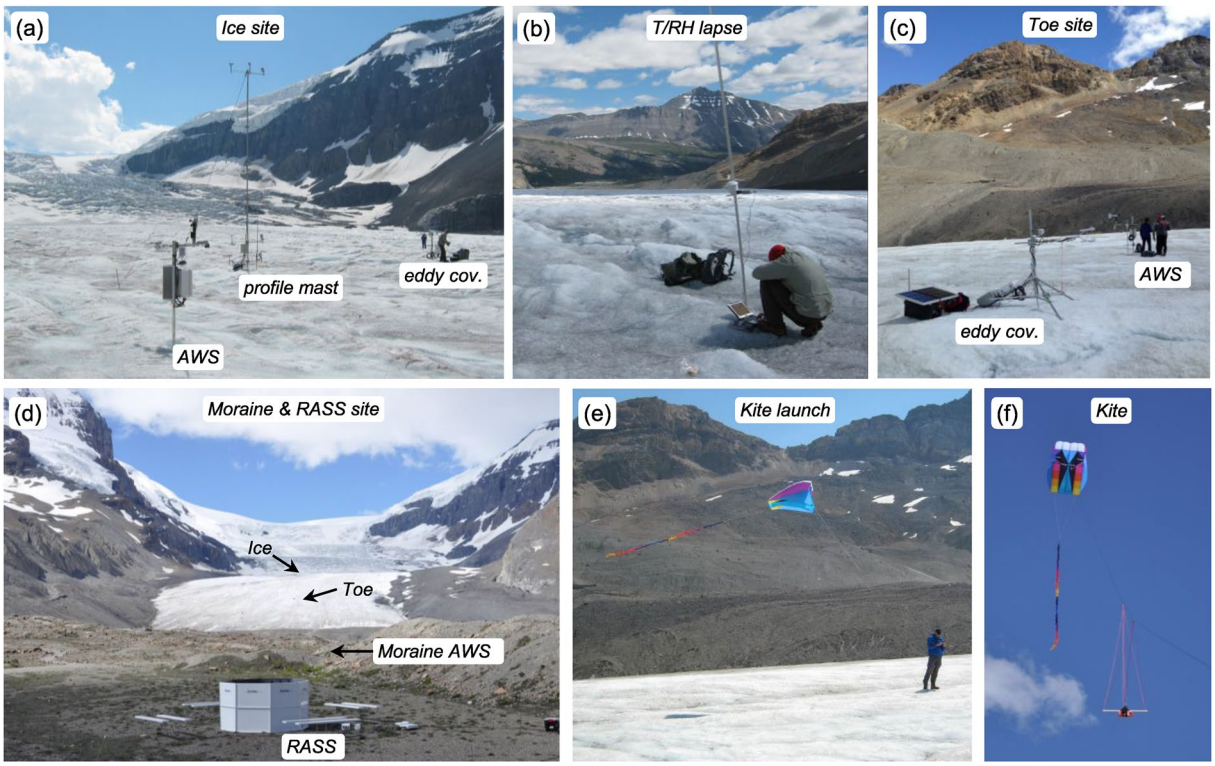

Figure 2. Photos of instrumentation deployed at (a) Ice site, (b) T/RH lapse rates sites, (c) Toe site, (d) Moraine and RASS site and (e), (f) kite profiling system. RASS, radio-acoustic sounding system.

2. Methods

2.1. Field Setting, Campaign Timeframe

Athabasca Glacier (52.19 N, 117.25 W) is an outlet glacier draining the Columbia Icefield, a large icefield (205.5 km^2 in 2009; Tennant & Menounos, 2013) astride the Continental Divide in the Canadian Rockies. The upper part of the glacier forms part of the main ice mass of the Columbia Icefield and consists of an extensive plateau at ~2,900 m a.s.l. and the south-western glaciated slopes of Snow Dome. After a series of steep icefalls, a relatively flat glacier tongue extends for 3 km in a north-easterly direction, with a slope of 3°–5° in the first 2 km and 5°–10° in the last 1 km.

An intensive field campaign was undertaken between June 17 and July 1, 2015 on the lower Athabasca Glacier. All instrumentation was operating over the 12-day period 18 to 29 June (inclusive), and this is herein referred to as the study period. Note that solar noon is around 1400 h LST during the study period.

2.2. Instrumentation

Two long-term automatic weather stations (AWS) are situated within the study area (installed in September 2014). One is an on-glacier site on the glacier tongue at around 2,175 m (Ice) and the other is an off-glacier site on proglacial moraine 1 km from the glacier terminus at 1,983 m (Moraine) (Figures 1 and 2). Several temporary sites were established for the intensive field campaign (Table 1). An additional full AWS site (Toe) was placed on-glacier 700 m from the terminus at 2,021 m. To capture along-glacier lapse rates, a series of temperature/humidity sensors in naturally ventilated shields were attached to glacier mass balance stakes positioned along the center line of the glacier tongue between 2,228 and 2,022 m. A radio-acoustic sounding system (RASS) was situated close to the Moraine site to measure wind velocity and air temperature in the ice-free valley. Additional instrumentation was deployed at the Ice AWS location, including an 8 m profile mast. Eddy-covariance measurements of turbulent heat fluxes were also made at Ice and Toe, as well as fine-wire thermocouple measurements of near-surface temperature gradients (0–2 m) and additional radiation

Table 1
Instrumentation Deployed During Campaign

Site name	Instruments (and heights)	Nominal heights
Ice AWS	Air temperature/humidity: Rotronics HC-03-XT in 9 plate shield	1.5 m
	Wind speed/direction: RM Young 05,103 AP	2.0 m
	Barometric pressure: Viasala PTB110 (CS106)	1.5 m
	Solar/longwave radiation: Kipp & Zonen CNR4	1.5 m
	Infrared surface temperature: SI-111	1.4 m
	Surface height change: SR50a	1.6 m
Ice Profile	Wind speed: MetOne 014A	0.75/1.5/3/4.5/6/8 m
	Air temperature/humidity: Rotronics HC2-03-XT in 9 plate shield	0.75/1.5/3/4.5/8 m
Ice Eddy-covariance	3-dimensional wind velocity, sonic air temperature: IRGASON infrared gas analyzer and sonic anemometer	1.5 m
Toe AWS	Air temperature/humidity: Rotronics HC2-03-XT in 9 plate shield	1.5 m
	Wind speed/direction: RM Young 05,103	2.0 m
	Solar/longwave radiation: Kipp & Zonen CNR4	1.5 m
	Infrared surface temperature: SI-111	1.4 m
	Surface height change: SR50	1.2 m
Toe Eddy-covariance	3-dimensional wind velocity, sonic air temperature: IRGASON infrared gas analyzer and sonic anemometer	1.5 m
	Barometric pressure: Viasala PTB110 (CS106)	1.5 m
Moraine AWS	Air temperature/humidity: Rotronics HC2-03-XT in 9 plate shield	2.80 m
	Wind speed/direction: RM Young 05103-AP	3.35 m
	Barometric pressure: Viasala PTB110 (CS106)	1.8 m
	Solar/longwave radiation: Kipp & Zonen CNR4	2.2 m
	Infrared surface temperature: SI-111	0.8 m
	Surface height change: SR50	2 m
	Rainfall: TB4	0.8 m
RASS	x, y, z wind velocities and air temperature: Scintec Flat Array MFAS with windRASS™ extension	10 m resolution returns from 40 to 500 m.
Along glacier T/RH lapse rates	Air temperature and humidity: Onset Hobo Pro v2 in 6 plate shield	1.5 m
Kite profiling	Kestrel 4000 Weather meter	Bin averaged into 10 m bins, from 10 to 200 m.
	Wind speed—25 mm impellor, start up speed 0.6 m/s, resolution 0.1 m/s, accuracy the larger of 3% of reading or 0.1 m/s.	
	Air temperature—externally mounted and thermally isolated precision thermistor, resolution 0.1 K and accuracy 0.5 K.	
	Barometric pressure—monolithic silicon piezoresistive sensor, resolution 0.1 hPa and accuracy 1.0 hPa	

Abbreviations: AWS, automatic weather stations; RASS, radio-acoustic sounding system.

measurements at Ice. For the sake of brevity, the eddy-covariance and fine-wire thermocouple observations will be addressed elsewhere. Further details of instrumentation at each site location are given in Table 1.

Melting of the glacier surface was substantial during the campaign, with 0.90 m of melt recorded at Ice over 12 days. On the profile mast, the lower level sensors (0.75 and 1.5 m) were lowered daily to maintain heights close to their nominal heights, while the nominal heights for the upper level sensors are given as the average height over the 12-days study period. The Ice AWS, Toe AWS and along-glacier lapse rate sensors were lowered every 1–2 days through the study period to maintain their nominal heights.

Wind and temperature data from the NCEP/NCAR Reanalysis 1 700 hPa pressure level for the point 52.5°N 242.5°E was used to provide context for large-scale conditions (https://www.esrl.noaa.gov/psd/data/gridded/data.ncep.reanalysis.html). The mean height of the 700 hPa level during the study period was 3,110 m.

2.3. Kite Profiling

A kite-based profiling system was used to measure wind speed and temperature profiles in the lowest 200 m above the glacier. The system consisted of a 1.4 m^2 parafoil kite on single Dacron line with 60 kg breaking strain (Figure 2c). A Kestrel 4000 weather meter was attached to the kite line 10 m below the kite with a picavet system that kept the wind impellor facing the wind (Figure 2d). Flights were made periodically when wind conditions permitted. This was normally when the 2 m wind speed > 4 m s^{-1}. The maximum height obtained was limited by the wind speed and weight/drag of the system. Generally, 300 m of line was used to reach 200 m above the surface. Before a sounding was made, the line was set out and tethered, allowing the kite to be raised and lowered above the same location by walking the line up and down.

A sounding consisted of three ascents/descents over the space of 30 min. Wind speed, air temperature, and barometric pressure were logged every second by the Kestrel. Height was derived from the barometric pressure. Ascent/descent speed was reduced in the 30 m closest the surface to allow the sensors sufficient time to respond to the rapid change in temperature. Comparison of temperature profiles during ascent and descent confirmed the temperature sensor observations were not impacted by response times. However, the response time of the relative humidity sensor was too slow compared to the ascent/descent rates, and these measurements were not used.

2.4. Data Processing

Temperature measurements made in the passively ventilated RM Young Gill shields on Ice and Toe AWS were corrected for solar heating using the expression of (Huwald et al., 2009; Figure 8b) with coefficients ($a = 1.9$, $b = 0.4$) determined locally with comparison to a humidity-corrected sonic temperature from a co-located sonic anemometer, as recommend. Sensor malfunction resulted in the intermittent loss of wind speed data from 1.5 m on the profile mast. Data from these periods (81.5 h) were replaced by wind speed measured at 1.5 m by the sonic anemometer on the co-located eddy-covariance system. Rapid ice surface melting caused the sensor arm at Toe AWS to rotate during the study period so wind direction from the sonic anemometer at Toe is used.

The RASS data were processed into 30-min averages to align with the AWS data using the APrun software package (version 1.46, Scintec AG, Germany). Diurnal mean wind velocities presented in Figures 5a and 5b were rotated so the *Ux* wind was aligned with the glacial valley (35°East of North), so that positive *Ux* represents down-glacier flow and *Uy* represents cross-glacier flow from right to left when looking down-glacier. Virtual air temperature profiles were not retrieved from RASS measurements during the afternoons of 27 and 28 June, so diurnal averages presented in Figure 5c are for 22 to 26 June.

Kite profile data were post-processed into 10 m altitude bins, averaging all data ± 5 m from 10 to 200 m altitudes.

Horizontal pressure gradient perturbations between Ice, Toe and Moraine were calculated by first removing the mean barometric pressure difference between each site, then dividing the remaining differences by the horizontal distance between each site (Ice to Toe: 1,730 m, Toe to Moraine: 1,410 m).

3. Results

3.1. Temporal Evolution of Meteorological Conditions

The temporal evolution of meteorology at key locations is detailed in Figure 3. After an unsettled period (18–20 June) with a subdued diurnal cycle in air temperature, a general warming trend was observed over the study period. A strong diurnal cycle of air temperature at off-glacier sites (Moraine and RASS at 50 m) was dampened at on-glacier sites (Ice and Toe). On-ice air temperatures at Ice and Toe are similar except for 20 and 21 June, where temperature is warmer at Toe, and 26 to 28 June where Toe was cooler in the late

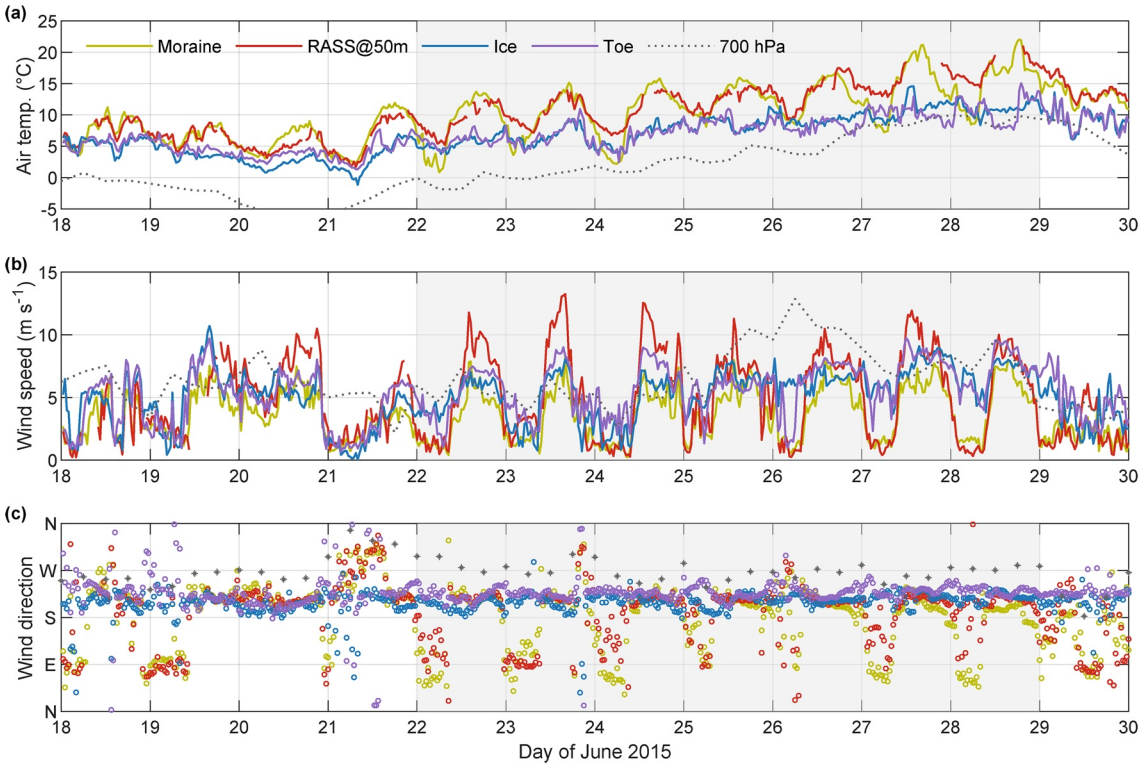

Figure 3. Air temperature, wind speed and direction at selected sites over the study period, 18 to 29 June, 2015. The shaded region (22–28 June) is defined as an IOP. The gray dots in panel (c) are the wind direction at 700 hPa. IOP, intensive observation period.

afternoon and evening by a few degrees. The period 22 to 28 June was a period of fair weather, exhibiting clear diurnal cycles in wind speed and air temperature along with persistent down-glacier winds and is termed the intensive observation period (IOP). During the IOP, the glacier surface temperature at Ice was at melting point, except for the early morning periods of 22–24 June. The predominately down-glacier winds at Ice and Toe show large diurnal variations in strength early in the IOP, then transition to moderate wind speed during the night-time from June 25 onwards. This transition is associated with an increase in nocturnal air temperature in the ice-free valley ABL greater than 10°C and a melting surface at Ice. The two off-glacier sites (Moraine and RASS) show a coherent and clear diurnal cycle in wind speed and direction throughout the IOP: weak winds from the east were observed during the early morning hours while strong south-westerly winds (down-glacier) dominated from mid-morning till midnight. Early in the IOP, wind speed during the afternoon is weaker at 2 m at on-glacier sites compared to the 50 m RASS measurements, while later in the IOP afternoon, wind speeds are similar between these sites and elevations. Reanalysis data at 700 hPa (Figures 3b and 3c) show a generally light westerly flow around 5–10 m s^{-1} throughout the study period, except for period of stronger winds on 25 and 26 June.

3.2. Near-Surface Profiles of Wind Speed and Temperature in the Glacier SBL

The typical diurnal cycle of wind speed and temperature profiles at the Ice site during the IOP (Figures 4a and 4c) displayed weaker gradients in the early morning hours, as expected from the colder temperatures observed. However, by 1200 h, stronger wind speeds and warmer air temperatures created strong gradients in wind speed and temperature close to the glacier surface. Strong gradients in temperature remained through the afternoon till 2400 h despite wind speed decreasing from late afternoon. Though no low-level wind speed maximum was observed in the average profiles, a wind speed maximum below 8 m (the highest measurement level) was observed during 25% of all 30-min periods during the IOP. Periods with a wind speed maximum at the lower measurement levels (0.75–3 m) were associated with markedly colder temperatures and lighter wind speeds than average (Figures 4b and 4d) and typically occurred during the

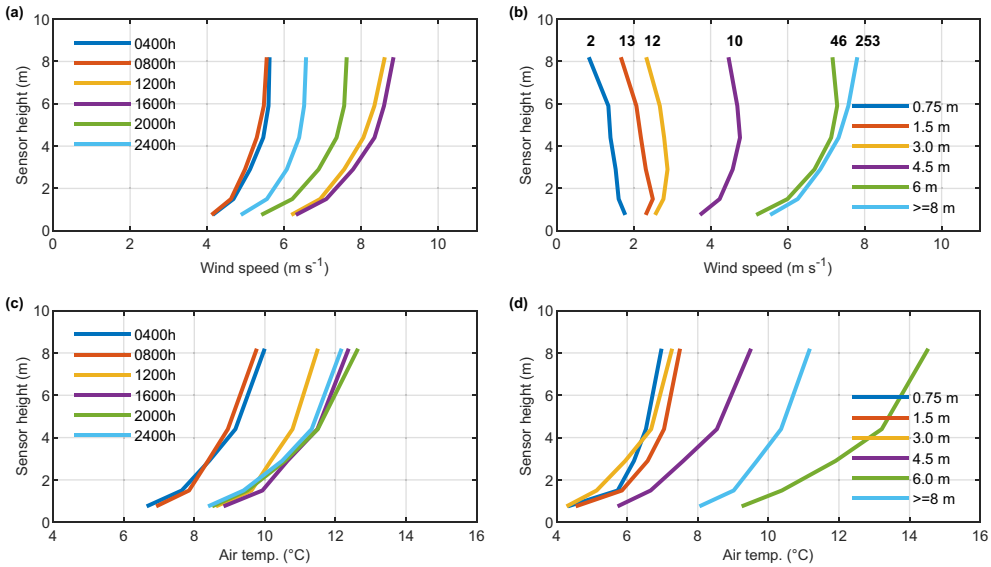

Figure 4. Mean wind speed and temperature profiles (left) for diurnal cycle and (right) during periods with wind speed maximum observed at different levels of mast during the IOP. Profiles are 30-min averages and the number of periods contributing to means in (b) and (d) are given above profiles in (b). IOP, intensive observation period.

early morning during the first part of the IOP. Periods where wind speed maximums were observed at higher measurement levels (4.5 to ≥8 m) were associated with progressively stronger winds and warmer air temperatures. The warmest average temperature profile was associated with a wind speed maximum at around 6 m, with cooler temperatures and weaker temperature gradients during periods with a wind speed maximum at or above 8 m. The dominance of periods with no observable wind speed maximum below 8 m contrasts with Stenning et al. (1981) who found 75% of profiles on Peyto Glacier had a wind speed maximum below 6 m, and van den Broeke (1997b) who found 75% of profiles had a wind speed maximum below 13 m on Pasterze during a period of abnormally warm weather. Note that the lack of an observed wind speed maximum in the profile data does not discount the possibility of one occurring at or above the highest measurement level. This should be kept in mind when comparing to the results of van den Broeke (1997b), which had a higher maximum profile observation height than the present study. A positive relationship between the strength of wind speed and the height of the wind speed maximum is expected from katabatic theory (Denby & Greuell, 2000) and for the typical wind speed at the Ice site during mid-afternoon, a wind speed maximum would be expected around or slightly above 8 m (Denby & Greuell, 2000; Figure 7, slope of 5° and maximum wind speed of 9 m s^{-1}). This underlines the need for measurements of wind speed and temperature above 8 m made using the kite profiling system that are presented later.

3.3. Diurnal Variation of Within-Valley ABL

A down-glacier breeze at the RASS site (indicated by positive *Ux* wind velocity and *Uy* close to zero) typically began at 0800 h and built in strength through to 1300 h LST (Figure 5a). During its onset, the breeze was consistent with height, though through the afternoon, stronger wind speeds were observed below 100 m above ground level. The period of strongest wind speeds lasted from 1300 to 1600 h, after which moderate wind speeds lingered into the evening, often associated with moderate winds from the west (indicated by negative *Uy*) above 50 m (Figure 5b). After midnight, down-glacier winds rapidly disappeared, and a light easterly was often observed (positive *Uy*). During the onset of the daytime breeze at 0800 h, the air temperature in the lowest 200 m increased rapidly, presumably associated with the transition from the nocturnal boundary layer (Figure 5c). From 0900 h warming was strongest at lower levels and the ABL continued to warm through to late afternoon. Increased temperature at higher levels (>100 m) around 2,000 h is perhaps associated with the weakening of down-glacier south-westerly breezes and change to moderate westerlies. Air temperature rapidly decreased around 2100 and 2400 h after which air temperature decreased slowly until a stable ABL developed in the early morning hours. The Ice profile mast (Figure 4) and RASS

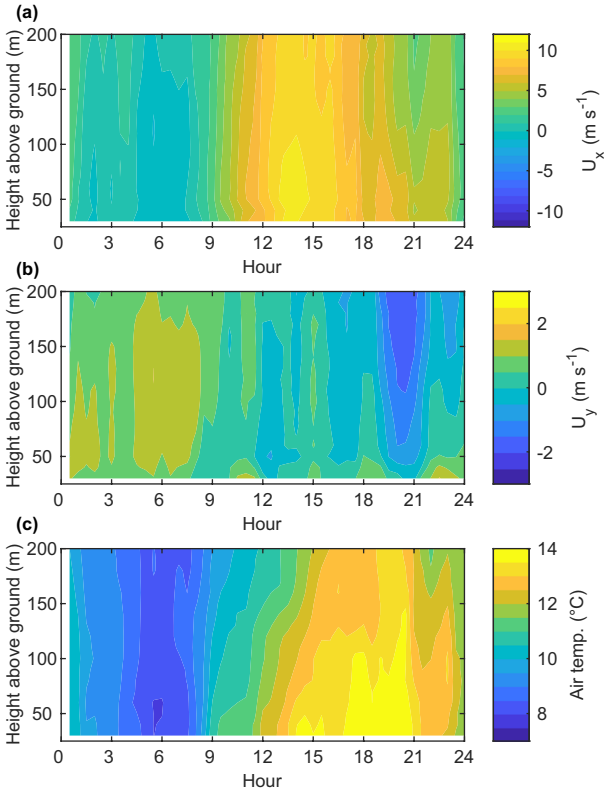

Figure 5. Mean diurnal cycle of (a) down-glacier (*Ux*) and (b) cross-glacier (*Uy*) wind velocity, and (c) air temperature above ice-free valley from RASS during IOP. Note that *Ux* and *Uy* have different *z* scales. IOP, intensive observation period; RASS, radio-acoustic sounding system.

data point to a coherent diurnal circulation that spans the glacier and pro-glacial area, characterized by increasing temperature and down-glacier wind speed during the morning, peak wind speeds in the early to mid-afternoon and warm temperatures that persist late into the evening.

3.4. Kite Profiling of Glacier ABL

Kite flights were used to profile the glacier ABL during most afternoons, with flights alternating between the Ice and Toe sites (Figure 6). Light and/or variable winds on June 20 and 21 did not allow deep ABL profiles and revealed the flight limit of the kite profiling system to be around 4 m s^{-1} at 2-m height. There was good correspondence between the kite data at 10 m (averaged from 5 to 15 m) and the profile mast measurements at 8 m, which gives confidence in the system. Air temperature gradients during most flights indicated a predominately well-mixed atmosphere overlying a shallow surface layer around 20–30 m deep that was influenced by the glacier surface (e.g. June 24 1429 h Toe). In most flights, wind speeds from 20 to 200 m were constant or slightly increasing with height and exceeded that measured by the profile mast in the lowest 8 m. The most obvious exception to this was the afternoon of June 28 in which a maximum wind speed occurred at 6 m height, with much lighter winds above. This, along with strong temperature gradients, is characteristic of a "glacier wind". Enhanced near-surface wind speeds were also observed during two morning flights (23 and 24 June) above Toe. The June 27 1623 h profile included a possible wind speed maximum between 10 to 20 m, along with large fluctuations in wind speed, compared to other afternoon flights. The June 27 1623 h profile was characterized by strongly fluctuating air temperature between 40 and 80 m and an extremely stable profile up to 90 m. During this flight time, strong down-glacier cooling was also observed, with Toe markedly cooler than Ice (Figure 3a). The dissimilarity of glacier ABL profiles suggests multiple mechanisms play a role in forcing the observed diurnal circulation. The availability of multiple kite ABL profiles on 24 and 28 June permitted in depth case studies of these two days to explore diurnal variations in glacier ABL, valley circulation and glacier SBL in more detail.

3.5. Case Studies: "Icefield Breeze" Versus "Glacier Wind"

3.5.1. 24 June: "Icefield Breeze"

During the morning of June 24, wind speed profiles indicated a light down-glacier nocturnal flow with a low wind speed maximum at 1.5 m (Figure 7c). This nocturnal flow persisted at Toe during the 1013 h flight (Figure 7a). At this time, calm or light easterly winds (2–3 ms^{-1}) were observed above the ice-free valley by the RASS (Figure 7b). Down-glacier lapse rates in the morning showed moderate cooling from the icefall to mid-glacier and warming on the lower glacier tongue that slightly exceed the dry adiabatic lapse rate (Figure 7d).

The 1210 h Ice kite profile coincided with initiation of strong daytime down-glacier winds at the off-glacier sites (Figure 3b) and transition from nocturnal flow, as evidenced by large standard deviations of wind speed (Figure 6) and an isothermal temperature profile in the lowest 60 m (Figure 7a). Afternoon kite profiles at Toe and Ice displayed near-constant wind speeds from 20 to 200 m and a temperature profile indicating a well-mixed ABL above 20 m. Wind speed at 1.5 m strengthened down-glacier from Ice to Toe (Figure 3b), but 50 m RASS wind speed was much greater and a little stronger than wind speeds from similar heights in the glacier ABL kite profiles. The RASS velocities were aligned along the glacier tongue. The consistent wind speeds with height and extension of the strong winds into the ice-free valley suggest the mechanism responsible for the observed down-glacier winds was operating at a scale larger than the

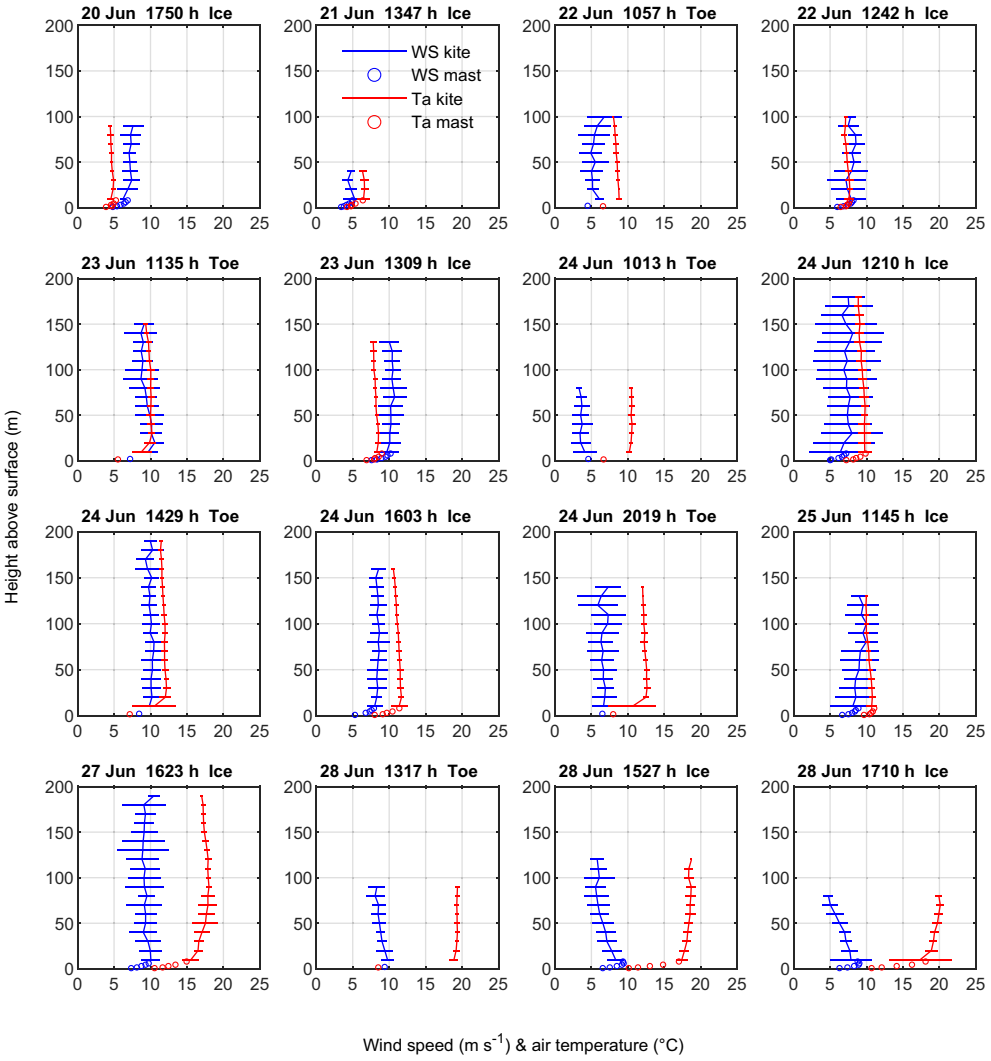

Figure 6. Profiles of wind speed (in blue) and temperature (in red) from all kite flights above Ice and Toe stations. Lines show mean and error bars show standard deviation of all kite measurements ±5 m from measurement height. Dots give mean values from Ice profile mast and Toe AWS during kite flights. AWS, automatic weather stations.

outlet glacier and can be thus thought of as having external forcing. While the mechanisms responsible for the observed circulation are discussed later, the term "icefield breeze" is used herein to describe the strong down-glacier winds that lack a wind speed maximum close to the surface, to distinguish these conditions from more typical "glacier wind" conditions and reflect their presumed origin in the Columbia Icefield.

During the afternoon period of "icefield breeze" conditions, air temperatures changed very little down the glacier tongue, indicating moderate down-glacier cooling was balanced by adiabatic warming, entrainment and/or advection of warm air into the SBL (Figure 7d).

3.5.2. June 28: "Glacier Wind"

During the morning of 28 June, RASS measurements indicated very similar conditions in the ice-free valley as the 24 June example just described, with calm or weak easterly winds (Figure 8b). However, on-glacier conditions contrasted sharply, with moderate wind speeds (~4–9 m s^{-1}) and no wind speed maximum < 8 m observable in the profile mast data (Figure 8c). Down-glacier lapse rates indicate much warmer temperatures than 24 June (10°C compared to 4°C at 2,230 m below the icefall), but a similar pattern of cooling from the icefall to mid-glacier and warming on the lower glacier tongue (Figure 8d).

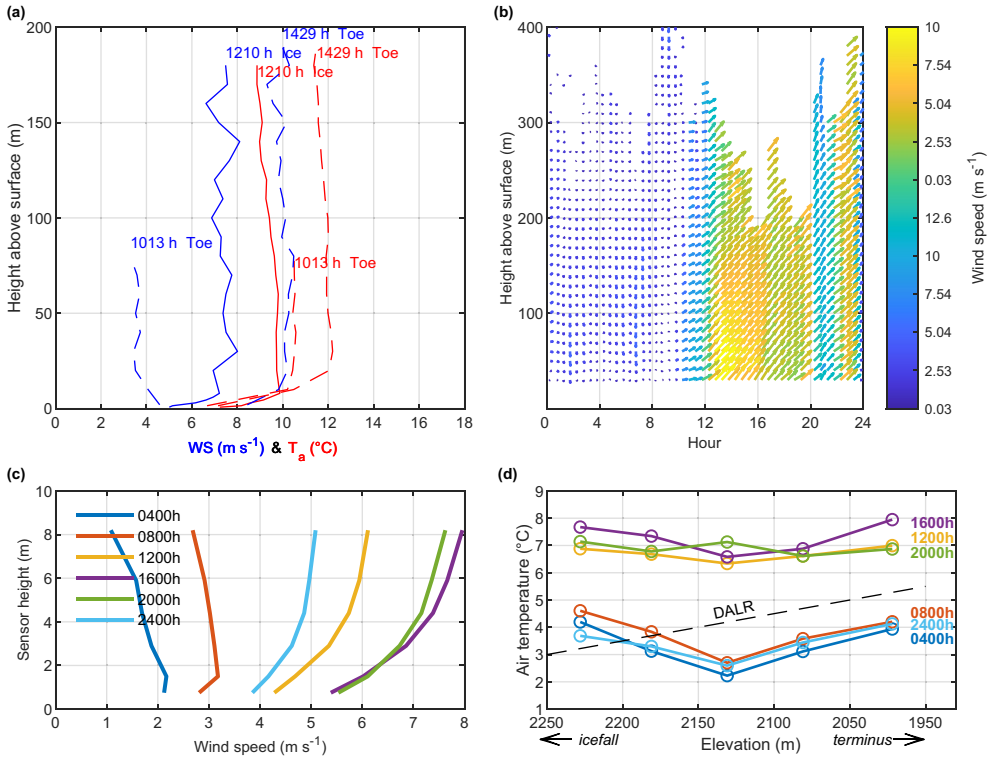

Figure 7. Case study on 24 June showing diurnal progression of (a) air temperature (in red) and wind speed (in blue) from periodic kite, mast and AWS observations above Ice (solid lines) and Toe (dashed lines), respectively, (b) wind speed and direction above RASS, (c) near-surface wind speed from profile mast at Ice, and (d) air temperature along the centerline of the glacier tongue, with the dry adiabatic lapse rate (DALR) for reference. Note 10 m bin is removed from Kite profiles at Ice for clarity. In panel (b) a northward wind vector is aligned up the page. AWS, automatic weather stations.

The onset of a daytime breeze at RASS at 0930 h (Figure 8b) was accompanied by increased wind speed at Ice and Toe (Figure 3b). After the morning transition, a strong down-glacier cooling developed from 0800 to 1200 h (Figure 8d). From 1200 to 1700 h strong down-glacier cooling was observed in the lapse rate data and a wind speed maximum at 6 m was observed at Ice. Kite flights at Toe and Ice indicate wind speed diminishes strongly with height, with this pattern becoming stronger during the afternoon in conjunction with warming in the ABL (Figure 8a). WindRASS data during afternoon kite flights show moderate winds coming from the glacier extending to 200 m (Figure 8b). In all kite flights, air temperature increased up to the maximum heights reached (80–120 m), indicating a very stable ABL. Similar to June 24, down-glacier wind speed increased from Ice to Toe (Figure 3b), but in contrast, wind speed in RASS profiles are similar to these on-glacier surface wind speeds (Figure 8b). These observations suggest a "glacier wind" driven by intense sensible heat exchange at the glacier surface (as confirmed by eddy covariance measurements [work in progress]) was the dominant mechanism on 28 June.

Between 1600 and 2000 h the strong down-glacier cooling was disrupted at the lowest site (Figure 8d). This disruption began at 1800 h (not shown) and propagated up-glacier over the next 2 h, resulting in a marked rise in air temperature at Toe from 8°C to > 15°C (Figure 3a). The intense down-glacier cooling and late-afternoon disruption extended to the Moraine site (Figure 3a). The wind direction at Toe (Figure 3c) indicates a shift to more westerly winds during the disruption, suggesting that advection of warmer air from surrounding terrain into the "glacier wind" may have been responsible. Wind direction from RASS did not show any large deviation during this period.

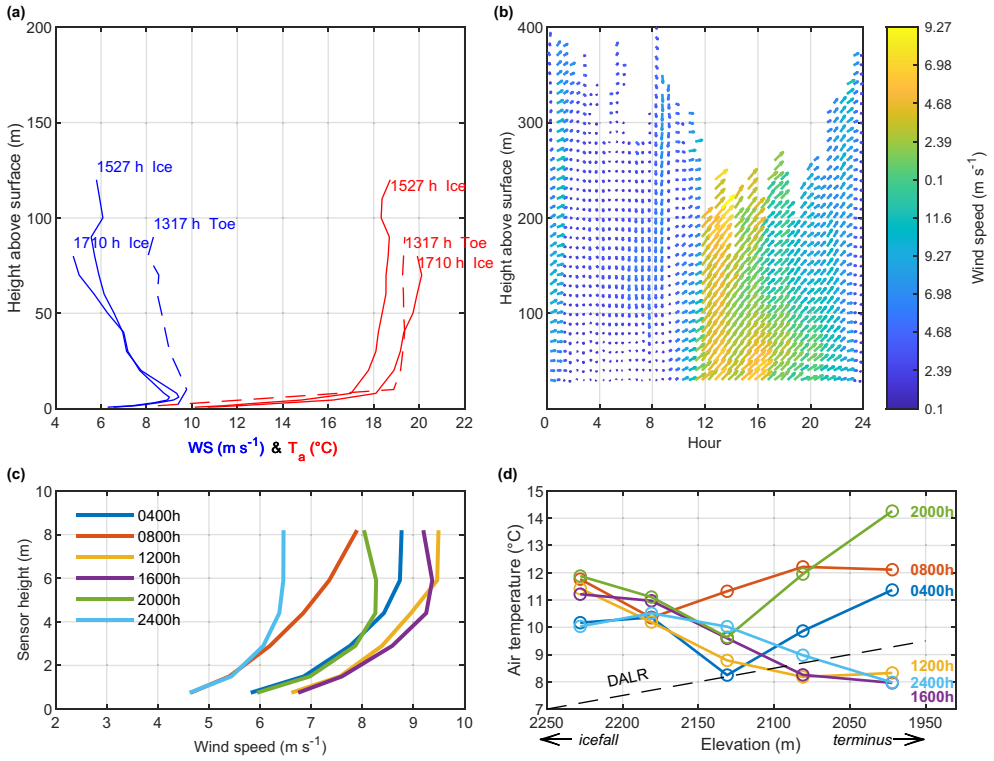

Figure 8. Same as Figure 7 but for June 28 case study.

3.6. Lapse Rate of Air Temperature Within Glacier SBL

The mean diurnal evolution of air temperature along the glacier tongue during the IOP was characterized a v shape with elevation with down-glacier cooling on the upper portion and a warming on the lower portion (Figure 9a). The site closest to the glacier terminus was consistently warmer than other sites, indicating the glacier SBL is more frequently disturbed by entrainment or advection. The magnitude of cooling on the upper and warming on the lower tongue intensified during the night. During the day, down-glacier cooling weakened but extended further down-glacier.

Periods with a wind speed maximum at or below 6 m, indicative of "glacier wind" or katabatic conditions display a stronger v shape than periods with no observable wind speed maximum, which are likely to be dominated by external forcing (including icefield breezes) (Figure 9b; compare gray and blue lines showing

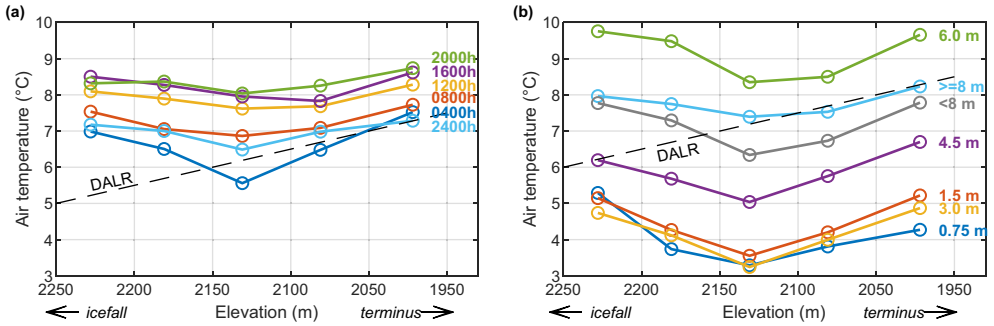

Figure 9. Evolution of air temperature down the centerline of the glacier tongue during the IOP: (a) mean diurnal cycle (b) during periods with wind speed maximum at different levels of profile mast at Ice. The light blue line in (b) shows mean evolution during periods where a wind speed maximum cannot be identified in the profile mast data (i.e. maximum recorded wind speed is at 8 m height). For the number of observation periods in panel (b) refer to Figure 4b. IOP, intensive observation period.

periods with wind speed max < 8 m and ≥8 m, respectively). The cooling between the first and third along-glacier T/RH sites is 1.4°C for periods with an identifiable near-surface wind speed maximum, and only 0.6 for periods with no observed wind speed maximum, despite similar average air temperature. This suggests the SBL on the upper tongue is more disrupted during periods of external forcing compared to "glacier wind" situations. The disruption inhibits down-glacier cooling of the SBL, which in turn also limits the potential for warming by entrainment on the lower tongue. A comparison of down-glacier cooling from the first to third sites on the case study days supports this idea, with less than 1°C cooling on the afternoon of the "icefield breeze" day (Figure 7d) but up to 2.5°C on the afternoon of the "glacier wind" day (Figure 8d). The stronger down-glacier cooling on the 28th is likely also a function of the warmer air temperatures in the valley core, which act to increase temperature deficit and drive increased sensible heat flux losses and buoyancy driven flow. The stronger down-glacier cooling appears to inhibit warming on the lower tongue till late in the day and produce very large increases in air temperature when the SBL was disrupted. In general, the observed down-glacier temperature profiles do not fit the concept of linear lapse rates, and further studies should consider the influence of advection and entrainment along with katabatic cooling cf. (Greuell & Böhm, 1998; Petersen et al., 2013; Petersen & Pellicciotti, 2011) for different wind regimes.

4. Discussion

While a full explanation of the mechanisms driving the observed "icefield breeze" warrants a thorough investigation using high-resolution meteorological modeling (e.g., Ma et al., 2013), some of the features of the observed circulation are discussed here to generate hypotheses.

Previous observations of the ABL in "glacier wind" conditions show that during the daytime, wind speed decreases to a minimum between 50 and 120 m above surface and becomes up-glacier above (van den Broeke, 1997b). The data collected during this campaign give no evidence for up-glacier flow above the glacier, nor the anabatic day-time winds expected at sites in the ice-free valley. A clear limitation of the kite profiling system is that it cannot fly when down-glacier winds are overlain by up-glacier return-flow. However, during periods of "glacier winds" in which wind speeds decreased toward the top of the kite profiles (i.e., 28 June), moderate down-glacier winds were observed through the whole RASS profile to 200 m. Therefore, it seems unlikely that an up-glacier return-flow overlaid the "glacier wind," at least in the lowest 200 m.

Strong daytime down-valley winds have been observed well beyond the glacierized extent down-valley from Mt Everest (Zhu et al., 2006). These winds develop from midday to midnight and extend through the entire valley ABL to 1000 m above the ground. Numerical modeling has suggested the primary mechanism for these winds is the development of along-valley potential temperature gradients as ice-free valley surface heats during the daytime (Song et al., 2007). The strong potential temperature gradients give rise to horizontal pressure gradients that drive the observed down-valley winds. Over glacier surfaces, wind speed is further increased by sensible-heat exchange at the glacier surface. The down-valley wind is balanced by an overall downward movement of air from higher levels of the atmosphere that plays an important role in the transport of ozone-rich air into the valley (Cai et al., 2007). This contrasts with the observed up-slope flow over Pasterze Glacier (van den Broeke, 1997b). The observations near and over the Athabasca Glacier are more congruent with the Everest case, where down-valley flow extends throughout the ABL both above and down-valley from the glacier.

The development of along-valley pressure gradients by heating in the ice-free valley is supported by observations during the IOP. First, a clear diurnal cycle in horizontal pressure gradient perturbations occurred between AWS sites during the IOP (Figure 10a). These gradients are an order of magnitude larger (0.1 hPa km^{-1}) than typical synoptic pressure gradients (0.01 hPa km^{-1}). The horizontal pressure gradients also extended from the Toe to the Moraine site, though they weaken during the evening. The diurnal cycle of pressure gradients corresponds with the diurnal cycle of on-glacier wind speed, which increased from 0900 to 1300 h and slowly weakened during the afternoon and evening (Figure 10b).

The on-glacier horizontal pressure gradients are also related very strongly ($r = -0.83$) to air temperature in valley ABL (Figure 11a) which is, in turn, related strongly to on-glacier wind speed (Figure 11b; $r = 0.69$). Horizontal pressure gradient perturbations are related more strongly to wind speed at Toe ($r = 0.74$) than Ice ($r = 0.60$), perhaps indicating a stronger influence of "glacier wind" at the Ice site.

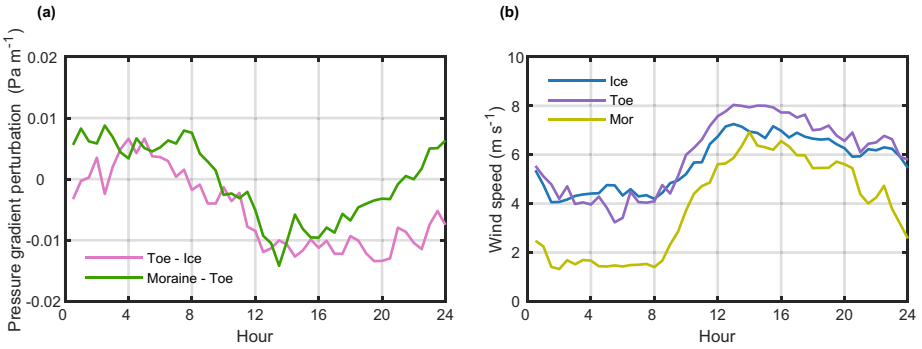

Figure 10. Mean diurnal cycle of (a) perturbations from average horizontal pressure gradient between AWS sites and (b) wind speed during the IOP. Pressure gradient perturbations are calculated with respect to the mean pressure gradient between AWS sites. Negative pressure perturbations indicate lower pressure at the site further down-valley. AWS, automatic weather stations; IOP, intensive observation period.

Other mechanisms beyond sensible heat exchange and mesoscale thermal contrasts may also play a role in forcing the observed icefield breezes. The Athabasca Glacier drains the Columbia Icefield (Figure 1) and this large glaciated surface is likely to cool the near-surface air and generate subsidence aloft, perhaps further enhancing the surface pressure gradients between icefield and the surrounding ice-free terrain by modifying the airmass upstream of the Athabasca Glacier. The Columbia Icefield also sits on the continental divide, exposed to the prevailing westerly geostrophic airflow. Thus, it is possible that topographic channeling or down-slope flow forced by large-scale westerly winds play a role in generating the observed circulation. Down-slope winds are associated with subsidence which produces warming and drying (Whiteman, 2000), which would help enhance the thermal contrast between the well-mixed valley ABL and the glacier SBL.

During the IOP, large-scale winds at 700 hPa were generally weaker than valley/glacier wind speeds during the afternoon, but channeling of large-scale winds and/or dynamically forced downslope wind associated with descending air in lee of icefield cannot be excluded. It is likely that the large-scale gradient wind had an influence on the morning of 25 and 26 June as the usual temperature inversion did not form between the Moraine surface-level site and RASS at 50 m (Figure 3) and the RASS vectors show that strong winds propagate downward toward the surface during the morning (not shown). On 27 and 28 June, RASS observations show that the strong daytime winds propagate upward during their onset (Figure 8b) and the kite profiles on 28 show wind speed decreasing with height, making it unlikely that the gradient wind is the primary mechanism on these days. The predominant westerly flow over the icefield may play a role in removing the pressure gradients that cause the elevated up-valley return flow in classical glacier wind theory and as observed over Pasterze. Mesoscale meteorological simulations may help to understand the extent to which each of these processes contributes to the observed diurnal wind system, and future work should explore this avenue. Mesoscale simulations may also help understand to what extent the presence of

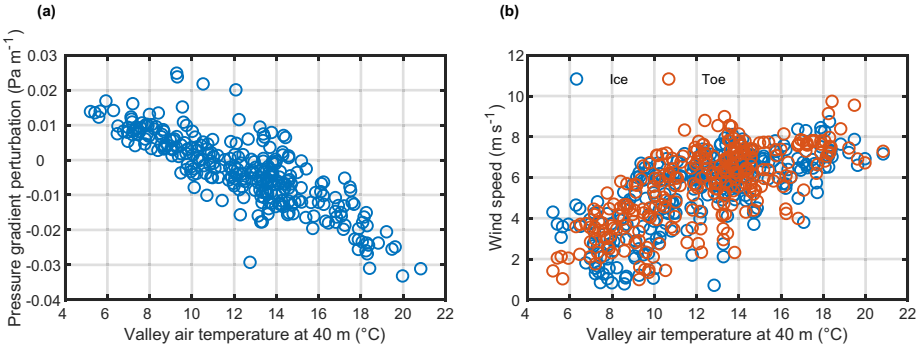

Figure 11. Relationship between air temperature at 40 m above RASS and (a) perturbation from average pressure gradient between Toe and Ice sites and (b) wind speed at on-glacier sites during the IOP. IOP, intensive observation period; RASS, radio-acoustic sounding system.

the icefield upwind alters melt rates and contributes to the survival of low-lying areas of the outlet glaciers under climate change.

While the balance of different forcing is currently uncertain, the observed daytime "icefield breezes" are likely to be driven by a mix of sensible heat driven cooling at the glacier surface and external forcing operating at a mesoscale or greater. Thus, budgets of momentum, heat and moisture with the ABL are likely to differ from those in classical "glacier wind" situations (cf. van den Broeke, 1997a). This also implies that care should be taken when using purely katabatic "glacier wind" frameworks to model SBL climates (e.g., Greuell & Böhm, 1998) and turbulent heat fluxes at mountain glacier surfaces (e.g., Oerlemans & Grisogono, 2002).

The patterns of glacier centerline temperature observed on Athabasca Glacier display a similar pattern to that observed on other mountain glaciers, with predominately down-glacier cooling on the upper sections and decreased cooling or warming on the lower glacier (e.g., Petersen et al., 2013; Troxler et al., 2020). The observed down-glacier warming on the lower tongue during periods of disruption is in excess of DALR, indicating non-adiabatic processes are at work (i.e. entrainment of warmer air from the ABL and/or horizontal advection from areas surrounding the glacier). This is consistent with recent studies show that external influences on the SBL are a common feature of many mountain glaciers, especially in the lower ablation areas where the near-surface climate is more distinct from that in non-glaciated areas (e.g., Mott et al., 2020; Shaw et al., 2020). However, the areas influenced by down-glacier cooling and/or disruption through entrainment or advection are not constant in space or time and appear to vary with the mechanism driving the down-glacier winds. Future work should use detailed atmospheric models (e.g., Sauter et al., 2016) to resolve the influence of different processes on near-surface climate to provide guidance on methods to extrapolate. This would include exploring the spatial and temporal scales associated with different mechanisms, optimum methods to extrapolate on and off-glacier AWS records, and relevant processes to include in statistical downscaling of gridded climate products. Along with this, work to examine the spatial and temporal variations in turbulent fluxes of energy and momentum associated with different wind regimes is needed to determine the effect of changes in SBL climate on the surface energy balance and melt.

5. Conclusions

An intensive campaign to profile the ABL near and on the Athabasca Glacier outlet of the Columbia Icefield with novel kite and radio-acoustic systems showed a distinct diurnal circulation develops during fair weather. Despite the typical on-glacier meteorology—strong down-glacier winds and minimal diurnal temperature range—the glacier ABL structure was significantly different from that expected for "glacier winds" driven solely by sensible heat exchange at the glacier surface. During the afternoon, strong down-valley winds extended throughout the ABL above the glacier and extended well beyond into the ice-free terrain. While the mechanisms responsible for the observed circulation are uncertain, a well-defined mesoscale circulation developed between the icefield and valley in the absence of strong synoptic forcing. This previously undocumented circulation is likely to be driven by horizontal pressure gradients that arise from the thermal contrast between valley ABL and ice surfaces and is loosely termed an "icefield breeze." Cooling driven by sensible-heat losses at the glacier surface likely enhanced this mesoscale flow, with a near-surface wind speed maximum typical of "glacier wind" conditions being observed during the night and on some days.

Regardless of mechanism driving the observed down-glacier winds, a stable SBL formed over the glacier, resulting in lapse rates of air temperature along the centerline of the glacier tongue that differ markedly from the environmental lapse rate. The lapse rates are extremely variable in space and time and do not follow easy linear relationships with elevation due to interaction of katabatic down-glacier cooling and warming due to entrainment and/or advection into the glacier SBL. In conditions dominated by "glacier winds" with a wind speed maximum close to the surface, down-glacier cooling of SBL on the upper glacier tongue is greater and temperature increases during periods that the SBL on the lower glacier tongue are disrupted are much larger than during "icefield breeze" condition. During periods dominated by "icefield breezes," down-glacier cooling is weaker, and temperature varies little along the glacier flowline, despite similar mean wind speed at 1.5 m within the glacier SBL. These results raise a number of outstanding questions that have implications for our understanding of how surface meteorology and melting of outlet

glaciers will be altered by climate change. Future work should use the observational datasets as a testbed for modeling the mechanisms for and spatio-temporal variations in ABL/SBL climate and surface energy balance in complex glaciated terrain.

Data Availability Statement

The data presented in this manuscript is available at https://www.frdr-dfdr.ca/repo/handle/doi:10.20383/101.0281.

Acknowledgments
This research was supported by the Changing Cold Regions Network, Canada Foundation for Innovation, Canada Research Chairs, Global Institute for Water Security, Natural Resources Canada, Parks Canada, Brewster Transport, Natural Sciences and Engineering Research Council of Canada and the Royal Society of New Zealand Marsden Fund. Invaluable field support was provided by Bruce Johnson, May Guan, Angus Duncan, Dhiraj Pradhananga, Emily Anderson and Daniel Guenther of the Center for Hydrology in Canmore and Saskatoon.

References

Ayala, A., Pellicciotti, F., & Shea, J. M. (2015). Modeling 2 m air temperatures over mountain glaciers: Exploring the influence of katabatic cooling and external warming. *Journal of Geophysical Research: Atmosphere*, *120*(8), 3139–3157. https://doi.org/10.1002/2015JD023137

Bromwich, D. H., Parish, T. R., Pellegrini, A., Stearns, C. R., & Weidner, G. A. (1993). Spatial and temporal characteristics of the intense Katabatic winds at Terra Nova Bay, Antarctica. In *Antarctic meteorology and climatology: Studies based on automatic weather stations* (pp. 47–68). AGU. https://doi.org/10.1029/AR061p0047

Cai, X., Song, Y., Zhu, T., Lin, W., & Kang, L. (2007). Glacier winds in the Rongbuk Valley, north of Mount Everest: 2. Their role in vertical exchange processes. *Journal of Geophysical Research*, *112*(D11). https://doi.org/10.1029/2006JD007868

Carturan, L., Cazorzi, F., De Blasi, F., & Dalla Fontana, G. (2015). Air temperature variability over three glaciers in the Ortles-Cevedale (Italian Alps): Effects of glacier fragmentation, comparison of calculation methods, and impacts on mass balance modeling. *The Cryosphere*, *9*(3), 1129–1146. https://doi.org/10.5194/tc-9-1129-2015

Collier, E., Mölg, T., Maussion, F., Scherer, D., Mayer, C., & Bush, A. B. G. (2013). High-resolution interactive modeling of the mountain glacier–atmosphere interface: An application over the Karakoram. *The Cryosphere*, *7*(3), 779–795.

Denby, B., & Greuell, W. (2000). The use of bulk and profile methods for determining surface heat fluxes in the presence of glacier winds. *Journal of Glaciology*, *46*(154), 445–452. https://doi.org/10.3189/172756500781833124

Greuell, W., & Böhm, R. (1998). 2 m temperatures along melting mid-latitude glaciers, and implications for the sensitivity of the mass balance to variations in temperature. *Journal of Glaciology*, *44*(146), 9–20.

Greuell, W., Knap, W. H., & Smeets, C. J. P. P. (1997). Elevational changes in meteorological variables along a midlatitude glacier during summer. *Journal of Geophysical Research*, *102*(D22), 25941–25954.

Greuell, W., & Smeets, C. J. P. P. (2001). Variations with elevation in the surface energy balance on the Pasterze (Austria). *Journal of Geophysical Research*, *106*(D23), 31717–31727.

Hofer, M., Nemec, J., Cullen, N. J., & Weber, M. (2017). Evaluating predictor strategies for regression-based downscaling with a focus on glacierized mountain environments. *Journal of Applied Meteorology and Climatology*, *56*(6), 1707–1729. https://doi.org/10.1175/jamc-d-16-0215.1

Hoinkes, H. (1954). Beiträge zur Kenntnis des Gletscherwindes. *Archiv fur Meteorologie, Geophysik und Bioklimatologie, Serie B*, *6*, 36–53.

Huwald, H., Higgins, C. W., Boldi, M.-O., Bou-Zeid, E., Lehning, M., & Parlange, M. B. (2009). Albedo effect on radiative errors in air temperature measurements. *Water Resources Research*, *45*(8). https://doi.org/10.1029/2008WR007600

Jiang, Q., & Doyle, J. D. (2008). Diurnal variation of downslope winds in Owens valley during the Sierra Rotor experiment. *Monthly Weather Review*, *136*(10), 3760–3780. https://doi.org/10.1175/2008mwr2469.1

Litt, M., Sicart, J. E., & Helgason, W. (2015). A study of turbulent fluxes and their measurement errors for different wind regimes over the tropical Zongo Glacier (16°S) during the dry season. *Atmospheric Measurement Techniques*, *8*(8), 3229–3250. https://doi.org/10.5194/amt-8-3229-2015

Litt, M., Sicart, J. E., Six, D., Wagnon, P., & Helgason, W. D. (2017). Surface-layer turbulence, energy balance and links to atmospheric circulations over a mountain glacier in the French Alps. *The Cryosphere*, *11*(2), 971–987. https://doi.org/10.5194/tc-11-971-2017

Ma, S., Zhou, L., Zou, H., Zhang, M., & Li, P. (2013). The role of snow/ice cover in the formation of a local Himalayan circulation. *Meteorology and Atmospheric Physics*, *120*(1–2), 45–51.

Martin, S. (1975). Wind regimes and heat exchange on glacier De Saint-Sorlin. *Journal of Glaciology*, *14*(70), 91–105.

Mott, R., Stipserki, I., & Nicholson, L. (2020). Spatio-temporal flow variations driving heat exchange processes at a mountain glacier. *The Cryosphere*, *14*, 4699–4718.

Munro, D. S., & Davies, J. A. (1977). An experimental study of the glacier boundary layer over melting ice. *Journal of Glaciology*, *18*(80), 425–436.

Oerlemans, J., Björnsson, H., Kuhn, M., Obleitner, F., Palsson, F., Smeets, C. J. P. P., et al. (1999). Glacio-meteorological investigations on Vatnajökull, Iceland, summer 1996: An overview. *Boundary-Layer Meteorology*, *92*, 3–26.

Oerlemans, J., & Grisogono, B. (2002). Glacier winds and parameterisation of the related surface heat fluxes. *Tellus A*, *54A*, 440–452.

Ohata, T. (1989). Katabatic wind on melting snow and ice surfaces (I) stationary glacier wind on a large maritime glacier. *Journal of the Meteorological Society of Japan. Series. II*, *67*(1), 99–112.

Parish, T. R., & Bromwich, D. H. (1989). Instrumented aircraft observations of the Katabatic wind regime near Terra Nova Bay. *Monthly Weather Review*, *117*(7), 1570–1585.

Parish, T. R., & Bromwich, D. H. (2007). Reexamination of the near-surface airflow over the Antarctic continent and implications on atmospheric circulations at high southern latitudes. *Monthly Weather Review*, *135*(5), 1961–1973.

Petersen, L., & Pellicciotti, F. (2011). Spatial and temporal variability of air temperature on a melting glacier: Atmospheric controls, extrapolation methods and their effect on melt modeling, Juncal Norte Glacier, Chile. *Journal of Geophysical Research*, *116*(D23). https://doi.org/10.1029/2011JD015842

Petersen, L., Pellicciotti, F., Juszak, I., Carenzo, M., & Brock, B. (2013). Suitability of a constant air temperature lapse rate over an Alpine glacier: Testing the Greuell and Böhm model as an alternative. *Annals of Glaciology*, *54*(63), 120–130.

Poulos, G., & Zhong, S. (2008). An observational history of small-scale Katabatic winds in mid-latitudes. *Geography Compass*, *2*(6), 1798–1821.

Radić, V., Menounos, B., Shea, J., Fitzpatrick, N., Tessema, M. A., & Déry, S. J. (2017). Evaluation of different methods to model near-surface turbulent fluxes for a mountain glacier in the Cariboo Mountains, BC, Canada. *The Cryosphere*, *11*(6), 2897–2918.

Reuder, J., Ablinger, M., Ágústsson, H., Brisset, P., Brynjólfsson, S., Garhammer, M., et al. (2012). FLOHOF 2007: An overview of the mesoscale meteorological field campaign at Hofsjökull, Central Iceland. *Meteorology and Atmospheric Physics*, *116*(1–2), 1–13.

Sauter, T., & Galos, S. P. (2016). Effects of local advection on the spatial sensible heat flux variation on a mountain glacier. *The Cryosphere*, *10*(6), 2887–2905.

Shaw, T. E., Brock, B. W., Ayala, Á., Rutter, N., & Pellicciotti, F. (2017). Centerline and cross-glacier air temperature variability on an Alpine glacier: Assessing temperature distribution methods and their influence on melt model calculations. *Journal of Glaciology*, *63*(242), 973–988.

Shaw, T. E., Yang, W., Ayala, Á., Bravo, C., Zhao, C., & Pellicciotti, F. (2021). Distributed summer air temperatures across mountain glaciers in the south-east Tibetan Plateau: Temperature sensitivity and comparison with existing glacier datasets. *The Cryosphere*, *15*(2), 595–614. https://doi.org/10.5194/tc-15-595-2021

Shea, J. M., & Moore, R. D. (2010). Prediction of spatially distributed regional-scale fields of air temperature and vapor pressure over mountain glaciers. *Journal of Geophysical Research*, *115*(D23). https://doi.org/10.1029/2010JD014351

Sicart, J.-E., Litt, M., Helgason, W., Tahar, V. B., Chaperon, T., Chaper, et al. (2014). A study of the atmospheric surface layer and roughness lengths of the high-altitude tropical Zongo glacier, Bolivia. *Journal of Geophysical Research: Atmosphere*, *119*, 3793–3808. https://doi.org/10.1002/2013JD020615

Smeets, C. J. P. P., Duynkerke, P. G., & Vugts, H. F. (1998). Turbulence characteristics of the stable boundary layer over a mid-latitude glacier. Part I: A combination of katabatic and large-scale forcing. *Boundary-Layer Meteorology*, *87*, 255–260.

Smeets, C. J. P. P., Duynkerke, P. G., & Vugts, H. F. (2000). Turbulence characteristics of the stable boundary layer over a mid-latitude glacier. Part II: Pure katabatic forcing conditions. *Boundary-Layer Meteorology*, *97*, 73–107.

Song, Y., Zhu, T., Cai, X., Lin, W., & Kang, L. (2007). Glacier winds in the Rongbuk Valley, north of Mount Everest: 1. Meteorological modeling with remote sensing data. *Journal of Geophysical Research*, *112*(D11). https://doi.org/10.1029/2006JD007867

Stenning, A. J., Banfield, C. E., & Young, G. J. (1981). Synoptic controls over Katabatic layer characteristics above a melting glacier. *Journal of Climatology*, *324*, 309–324.

Streten, N. A., & Wendler, G. (1968). Some observations of Alaskan glacier winds in midsummer. *Arctic*, *21*(2), 98–102.

Tennant, C., & Menounos, B. (2013). Glacier change of the Columbia Icefield, Canadian Rocky Mountains, 1919–2009. *Journal of Glaciology*, *59*(216), 671–686.

Troxler, P., Ayala, Á., Shaw, T. E., Nolan, M., Brock, B. W., & Pellicciotti, F. (2020). Modeling spatial patterns of near-surface air temperature over a decade of melt seasons on McCall Glacier, Alaska. *Journal of Glaciology*, *66*(257), 386–400.

van den Broeke, M. R. (1997a). Momentum, heat, and moisture budgets of the katabatic wind layer over a midlatitude glacier in summer. *Journal of Applied Meteorology*, *36*, 763–774.

van den Broeke, M. R. (1997b). Structure and diurnal variation of the atmospheric boundary layer over a mid-latitude glacier in summer. *Boundary-Layer Meteorology*, *83*, 183–205.

van den Broeke, M. R., Duynkerke, P. G., & Oerlemans, J. (1994). The observed Katabatic flow at the edge of the greenland ice-sheet during Gimex-91. *Global and Planetary Change*, *9*(1–2), 3–15.

van Lipzig, N. P. M., Turner, J., Colwell, S. R., & van Den Broeke, M. R. (2004). The near-surface wind field over the Antarctic continent. *International Journal of Climatology*, *24*(15), 1973–1982. http://dx.doi.org/10.1002/joc.1090

Whiteman, D. C. (2000). *Mountain Meteorology: Fundamentals and Applications*. Oxford: Oxford University Press.

Zhu, T., Lin, W., Song, Y., Cai, X., Zou, H., Kang, L., et al. (2006). Downward transport of ozone-rich air near Mt. Everest. *Geophysical Research Letters*, *33*(23). https://doi.org/10.1029/2006GL027726